

Open Research Online

The Open University's repository of research publications and other research outputs

Diffusion bonding of TiC or TiB reinforced Ti-6Al-4V matrix composites to conventional Ti-6Al-4V alloy

Journal Item

How to cite:

Prikhodko, Sergey V.; Savvakina, Dmytro G.; Markovsky, Pavlo E.; Stasuk, Olexander O.; Penney, James; Shirzadi, Amir A.; Davies, Peter D. and Davies, Helen M. (2020). Diffusion bonding of TiC or TiB reinforced Ti-6Al-4V matrix composites to conventional Ti-6Al-4V alloy. *Science and Technology of Welding and Joining* (Early access).

For guidance on citations see [FAQs](#).

© [not recorded]



<https://creativecommons.org/licenses/by-nc-nd/4.0/>

Version: Accepted Manuscript

Link(s) to article on publisher's website:

<http://dx.doi.org/doi:10.1080/13621718.2020.1751403>

Copyright and Moral Rights for the articles on this site are retained by the individual authors and/or other copyright owners. For more information on Open Research Online's data [policy](#) on reuse of materials please consult the policies page.

oro.open.ac.uk

Science and Technology of Welding and Joining

Diffusion Bonding of TiC or TiB Reinforced Ti-6Al-4V Matrix Composites to Conventional Ti-6Al-4V Alloy

--Manuscript Draft--

Manuscript Number:	STW5718	
Full Title:	Diffusion Bonding of TiC or TiB Reinforced Ti-6Al-4V Matrix Composites to Conventional Ti-6Al-4V Alloy	
Short Title:	Diffusion Bonding of TiC or TiB Reinforced Ti-6Al-4V Matrix Composites to Conventional Ti-6Al-4V Alloy	
Article Type:	Research Article	
Keywords:	diffusion bonding; titanium alloy; metal matrix composite; TiC; TiB; blended elemental powder metallurgy	
Corresponding Author:	Sergey Prikhodko, PhD University of California Los Angeles UNITED STATES	
Corresponding Author Secondary Information:		
Corresponding Author's Institution:	University of California Los Angeles	
Corresponding Author's Secondary Institution:		
First Author:	Sergey Prikhodko, PhD	
First Author Secondary Information:		
Order of Authors:	Sergey Prikhodko, PhD	
	Dmytro G. Savvakín	
	Pavlo E. Markovsky	
	Olexander O. Stasuk	
	James Penney	
	Amir A. Shirzadi	
	Peter D. Davies	
	Helen M. Davies	
Order of Authors Secondary Information:		
Abstract:	<p>The Diffusion Bonding of conventional alloy Ti-6Al-4V (Ti-64) and composites of this alloy with 10% of TiC or TiB fabricated using blended elemental powder metallurgy was successfully carried out at 850 to 1000 °C, with a holding time of 60 minutes under 0.7-1.5 MPa pressure. The metallographic and electron backscattered diffraction studies, as well as the bending and microhardness tests across the bonds are presented as the evidence of joint integrity. The selected experimental parameters do not cause undesirable structural changes (degradation) in the base metals adjacent to the bond interface. Particle reinforcement at ~10% did not appear to modify bonding parameters when compared to the unreinforced Ti-64 alloy.</p>	
Funding Information:	North Atlantic Treaty Organization (G5030)	Prof. Sergey Prikhodko

Diffusion Bonding of TiC or TiB Reinforced Ti-6Al-4V Matrix

Composites to Conventional Ti-6Al-4V Alloy

Sergey V. Prikhodko ^{a*}, Dmytro G. Savvakina ^b, Pavlo E. Markovsky ^b,
Olexander O. Stasuk ^b, James Penney ^a, Amir A. Shirzadi ^{c&d}, Peter D.
Davies ^e, Helen M. Davies ^e

^a Department of Materials Science and Engineering, University of California Los Angeles, Los Angeles, CA 90095, USA;

^b G.V. Kurdyumov Institute for Metal Physics, National Academy of Science of Ukraine, 36, Vernadsky Blvd., 03142, Kiev, Ukraine;

^c School of Engineering and Innovation, The Open University, Milton Keynes, MK7 6AA, UK;

^d Department of Materials Science and Metallurgy, University of Cambridge, Cambridge, CB3 0FS, UK;

^e Institute of Structural Materials, Swansea University Bay Campus, Crymlyn Burrows, Fabian Way, Swansea, SA1 8EN, UK

*corresponding author tel.: +1 (310) 825-9735; email: sergey@seas.ucla.edu

1
2
3
4
5
6
7
8
9
10
11
12
13
14
15
16
17
18
19
20
21
22
23
24
25
26
27
28
29
30
31
32
33
34
35
36
37
38
39
40
41
42
43
44
45
46
47
48
49
50
51
52
53
54
55
56
57
58
59
60
61
62
63
64
65

Diffusion Bonding of TiC or TiB Reinforced Ti-6Al-4V Matrix

Composites to Conventional Ti-6Al-4V Alloy

The Diffusion Bonding of conventional alloy Ti-6Al-4V (Ti-64) and composites of this alloy with 10% of TiC or TiB fabricated using blended elemental powder metallurgy was successfully carried out at 850 to 1000 °C, with a holding time of 60 minutes under 0.7-1.5 MPa pressure. The metallographic and electron backscattered diffraction studies, as well as the bending and microhardness tests across the bonds are presented as the evidence of joint integrity. The selected experimental parameters do not cause undesirable structural changes (degradation) in the base metals adjacent to the bond interface. Particle reinforcement at ~10% did not appear to modify bonding parameters when compared to the unreinforced Ti-64 alloy.

Keywords: diffusion bonding; titanium alloy; metal matrix composite; TiC; TiB; blended elemental powder metallurgy;

Introduction

Multi-layered structures have recently become very popular since they demonstrate a far advanced set of characteristics that combine different mechanical properties often non-compatible in a single layer structure [1]. Powder metallurgy (PM) is proven to be well-established cost-efficient way for the fabrication of layered structures made of Ti and its alloys, which is simply not possible using traditional cast and wrought technology.

Nevertheless, it is not always flawless. Sintering of compacts consisting of layers of heterogeneous composition can lead to cracking, bending, delamination of individual layers and other types of shape alteration due to differences in shrinkage of the different layer materials [2]. Residual porosity in PM products of Ti is another possible problem, which in some cases can adversely affect the mechanical properties and performance of

1 the structural components. Post-sintering, hot rolling or pressing are some customary
2 ways of reducing the porosity of Ti-based materials to an acceptable level, even near
3 zero if it is needed [3]. It was shown, however, that hot rolling could not be successfully
4 used on multi-layered structures due to the disparity in the plastic flows of different
5 layers [4]. Separate processing of individual layers to their best performance and post
6 processing bonding of the mating subcomponents is a credible pathway for fabrication
7 of the layered materials with highly optimized properties of each individual layer.
8
9

10
11
12
13
14
15
16
17 Over the past few decades Diffusion Bonding (DB) has become one of the well-
18 recognized joining techniques in metalworking, which is especially suited to the
19 fabrication of complex Ti-6Al-4V (Ti-64) structures [5]. DB is a solid-state and near-
20 net-shape joining process that is carried out well below the melting temperature of the
21 materials being bonded [6, 7]. The applied pressure is sufficient to assure intimate
22 interfacial contact but does not allow the macroscopic deformation of the parts [7]. The
23 deformation is normally confined primarily to surface asperities [8]. It also can be used
24 to joint parts made of different titanium alloys [9] or dissimilar alloying systems [10,
25 11]. Final mechanical properties of the joint are determined by the microstructure of the
26 bond interface, presence of defects, and microstructural changes that may occur in the
27 base metals adjacent to the bond interface. The mechanisms controlling diffusion
28 bonding have been extensively studied and the optimization of the key parameters that
29 govern the quality of the joint, namely temperature, time and pressure, have been
30 reported [12].
31
32
33
34
35
36
37
38
39
40
41
42
43
44
45
46
47
48
49

50
51 One of the major predicaments when bonding dissimilar alloys is optimization
52 of the bond parameters for two materials with very different physical and mechanical
53 properties. Additionally, some complications can arise due to presence of possible
54 contaminants such as oxides, second phase, etc. [13] and bond defects [9]. The bonding
55
56
57
58
59
60
61
62
63
64
65

1 of conventional Ti-64 alloy to a Ti-64 based composite was a primary interest of this
2 work. The presence of very hard and brittle reinforcement particles in one of the mating
3 subcomponents, makes the bonded materials dissimilar. The focus of this investigation
4 was on the evolution of interfacial microstructure and reliability of the joints.
5
6
7
8
9

10 **Materials and Methods**

11 *Samples preparation*

12
13 In this study DB was performed between the parts made of the alloy Ti-64 and two
14 different types of Ti- 64 based metal matrix composites. The first type of composite
15 contained TiC while the second one contained TiB; both having 10% (vol.) of
16 reinforcement particles. The bonding trials were performed using two different set-ups,
17 labelled in this study as Methods A and B. Cylinder samples Ø10×12 mm were used in
18 Method A and bars 65×10×10 mm were utilized in B. Bars were further machined to an
19 octagonal prism geometry approximately 59×9.2mm (the last is the diameter of the
20 circumscribed circle of the base) to facilitate their clamping, before the bonding.
21
22
23
24
25
26
27
28
29
30
31
32
33
34

35 Samples used for DB were fabricated using blended elemental powder
36 metallurgy (BEPM). Hydrogenated titanium (TiH₂) powder (3.5 % H, wt.) was used as
37 the base powder for fabrication. The TiH₂ powder particles size was < 100 µm. For Ti-
38 64 alloy samples powder of hydrogenated titanium was blended with 60%Al-40%V
39 master alloy powder (particles size < 63 µm). To fabricate the metal matrix composite
40 (MMC) samples, TiB or TiC in powder form were added to the blends and mixed
41 before the pressing. Size of TiC and TiB₂ powders were 1-30 µm and 5-30 µm,
42 respectively. The powder of TiB₂ expected to chemically transform during the sintering
43 following the in-situ reaction: TiB₂+Ti=2TiB. Blends for each sample were added to the
44 die before the pressing. Preform were pressed at 650 MPa using the die-pressing
45 protocol. Sintering of preforms was carried out in vacuum furnace at 1250 °C, for 4h
46
47
48
49
50
51
52
53
54
55
56
57
58
59
60
61
62
63
64
65

1 followed by the slow furnace cooling. As was reported earlier [2] such processing
2 provides dehydrogenation of titanium and formation of the bulk samples used for
3
4 subsequent diffusion bonding process.
5
6

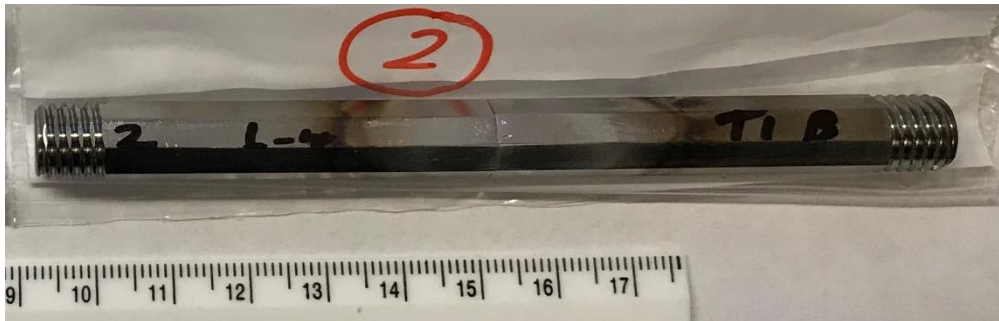
7 ***Diffusion bonding: Method A***

8
9
10 Cylindrical samples of both composites and conventional Ti-64 alloy were joined using
11
12 the diffusion bonder operating a 2-kW induction heating system. The bonding process
13
14 was carried out in vacuum of about 5×10^{-5} mbar. The joining faces of all samples were
15
16 ground with 1200 grit emery papers and rinsed in acetone just before loading in the
17
18 diffusion bonder. Temperature of each sample was monitored and controlled with a K-
19
20 type thermocouple spot-welded on one of the blocks, close to the joint. The bonding
21
22 temperature was between 850 to 900 °C when applying minimum 1 MPa bonding
23
24 pressure. The dwell time at the peak temperature was 60 min for all samples. Two
25
26 samples: one with TiB and another one with TiC composite were bond using identical
27
28 conditions in Method A, labelled TiB-A and TiC-A correspondingly.
29
30
31
32
33

34 ***Diffusion bonding: Method B***

35
36 To facilitate bonding in arrangement B the two specimens (the alloy and MMC) were
37
38 ground to a finish of 0.4 µm as part of the machining to form the final bonding samples.
39
40 No extra grinding was performed immediately before bonding. Then the specimens
41
42 were assembled in to the load train of a servo hydraulic frame via threaded collets. Both
43
44 faying surfaces were brought into contact and held under a holding force of 0.02 kN.
45
46 Bonding was performed in an argon atmosphere to shield the bond region from the local
47
48 environment. A water-cooled induction coil was placed around both specimens so that
49
50 the coil's hot zone aligned with the bond region. The bond region was heated to a
51
52 temperature of 1000 °C (+/- 5 °C) at a heating rate of approximately 5 °C sec and held
53
54 for 60 minutes at a stress of 0.7 MPa for regime #1, and 1.5 MPa for regime #2. On
55
56
57
58
59
60
61
62
63
64
65

1 completion, bonded specimens were air cooled to room temperature. Temperature
2 control was facilitated by N-type thermocouples welded to the surface of the TiB/TiC
3 specimens within 1mm of the faying surface. In total, four samples: two with TiB and
4 specimens within 1mm of the faying surface. In total, four samples: two with TiB and
5 two other with TiC composite were bond using conditions #1 and #2 in Method B,
6
7 labelled TiB-B1, TiB-B2, TiC-B1 and TiC-B2. A typical sample after DB is shown in
8
9 the Figure 1. The major difference between used Methods A and B was the closeness to
10
11 β -transus temperature of the alloy Ti-64 that is around $995\text{ }^{\circ}\text{C} \pm 20\text{ }^{\circ}\text{C}$, which provided
12
13 a different completion of the $\alpha \rightarrow \beta$ phase transformation. [14] The details of Method A
14
15
16
17
18
19



20
21
22
23
24
25
26
27
28
29
30
31
32
33
34
35
36
37
38
39
40
41
42
43
44
45
46
47
48
49
50
51
52
53
54
55
56
57
58
59
60
61
62
63
64
65
Figure 1. Sample TiB-B2 after DB. The area of the joint is in the middle of the rod. Slight oxidation is observed at about 15 mm distance on both sides from the interface between bond samples

and B can be found in references [15] and [16] correspondingly.

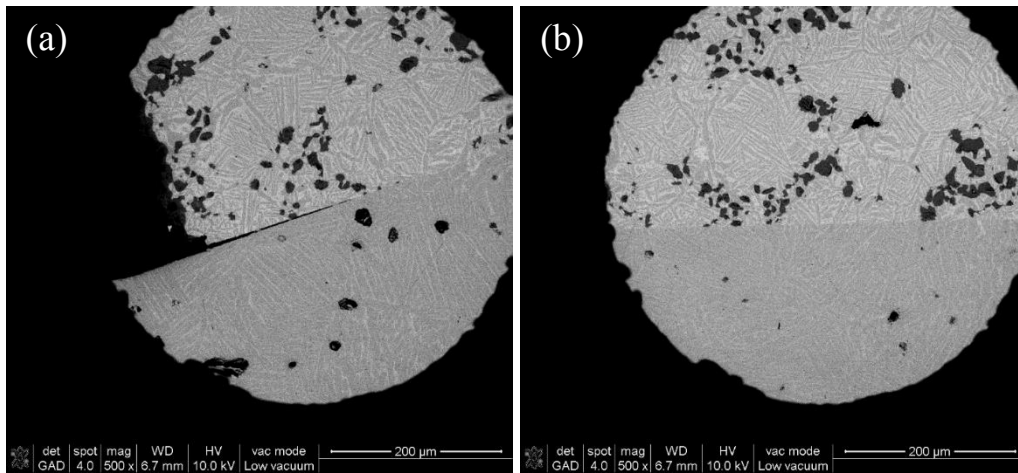
Structure characterization

Light optical microscopy (LOM) in this study was performed using M600 system (Nikon), IX70 (Olympus) and digital optical microscope VHX-1000 (Keyence). SEM study was conducted using variable pressure field emission gun SEM Nova 230 (ThermoFisher) equipped with EDS Noran 7 (ThermoFisher) and tungsten gun high vacuum SEM VEGA3 (Tescan). SEM study in secondary and backscattered electron modes were performed at 10-15 kV. EBSD-EDS study was conducted on the AZtec (Oxford Instruments) system coupled with the SEM LEO 1550VP (Zeiss) operated at 20 kV. Porosity of the samples was measured using the images taken of the polished samples. A number of ~1 mm thick slices were cut from the bonded samples prepared using

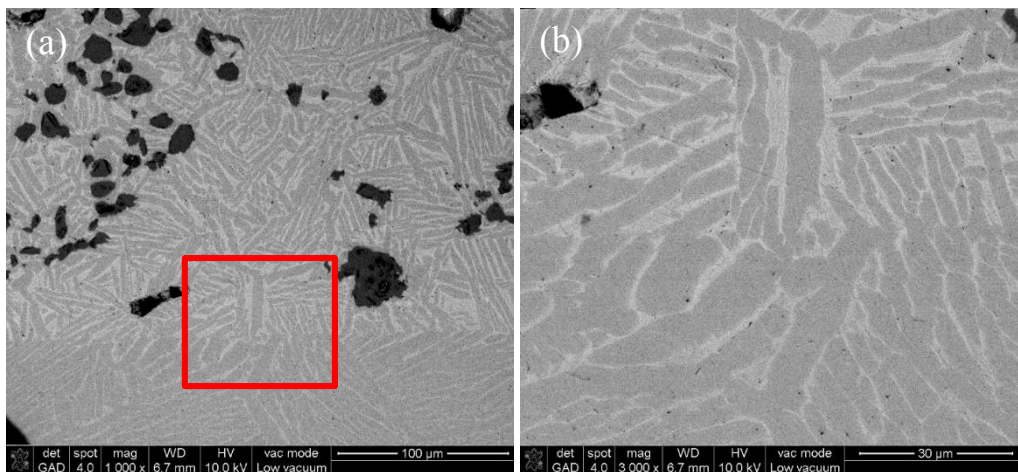
1 Method A and subjected to bending forces to assess the bond strength qualitatively.
2
3 Microhardness measurements were carried out using MicroMet® 2103 microhardness
4
5 tester (Buehler Ltd.) with a pyramid diamond tip. Two sets of measurements were taken
6
7 at loads 0.981 N across the bond interface near the center of the sample as well as at the
8
9 edge.
10

11 12 13 **Results and Discussion**

14
15 LOM and low magnification SEM images revealed formation of sound joints in all
16
17 samples bonded in 1 hour (Fig.2). Some defects were observed close to the edges of the
18
19 samples which are rather common in diffusion bonding. Such defects are caused by lack
20
21



36
37
38 Figure 2. Image of the sample TiC-A demonstrate some of macro defects of the bonding at
39
40 about 100-150 μm close to the edge of the sample (a), whereas rest of the sample reveal
41 consistency and no visible defects of the bonding along the interface (b).



58
59
60 Figure 3. SEM images of the interface resulted on DB of the TiC-A sample processed at
61
62 bonding temperature between 850 to 900 °C and 1 MPa bonding pressure. The area boxed
63
64 in (a) is shown in (b).
65

of full contact around the edges as a result of manual surface grinding prior to the bonding.

Higher magnification images demonstrate that almost defect-free interfaces were formed between all mating pairs at all processing parameters (Fig.3 and Fig.4). The interface clearly visible at relatively lower magnification images (Fig.3 (a) and Fig.4 (a, c)) becomes practically unrecognizable at higher magnification (Fig.3 (b) and Fig.4 (b, d)).

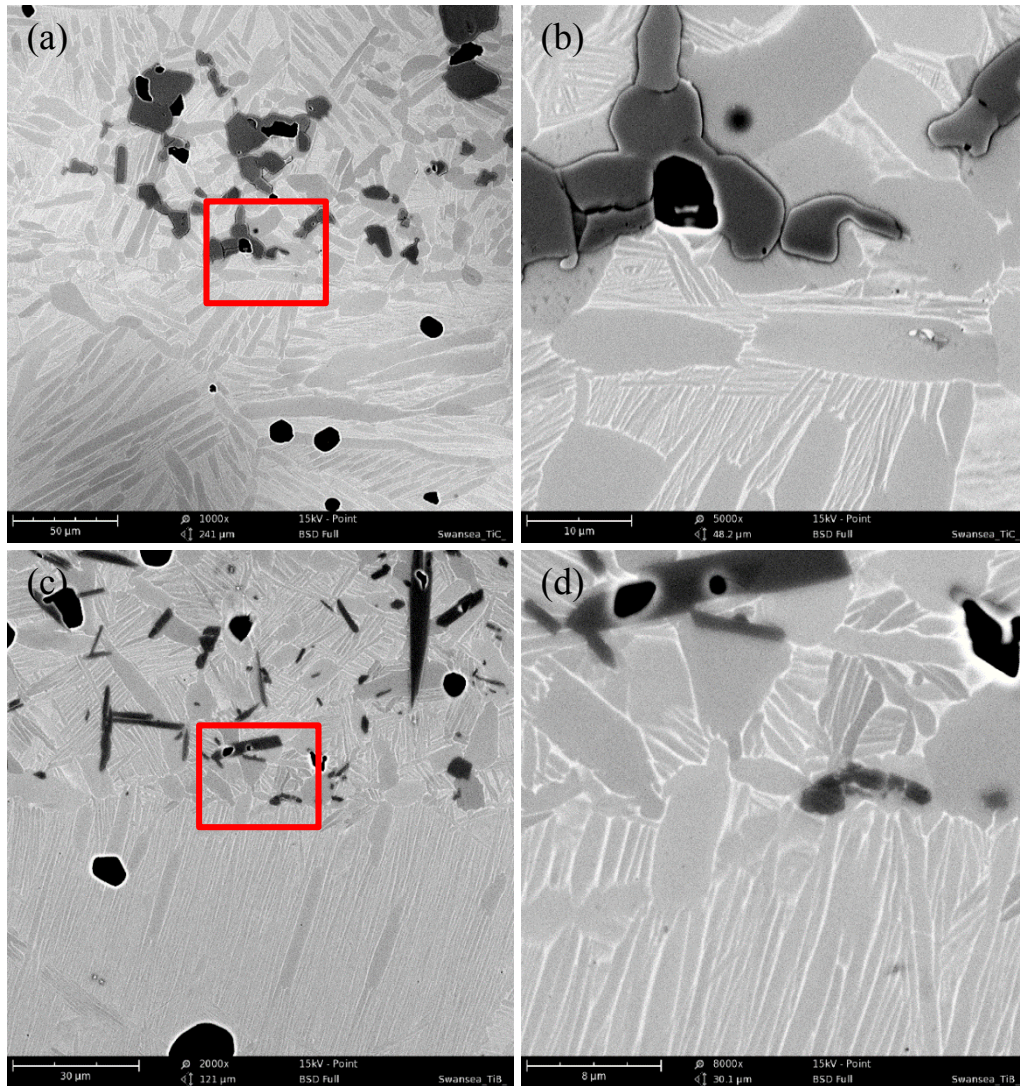


Figure 4. Images of the bond area of the TiC-B2 (a, b) and TiB-B2 (c, d) processed at 1000 °C for 60 minutes at a stress of 1.5MPa. Images (b) and (d) shows boxed areas in (a) and (c) correspondingly.

It is evident that the interface is not completely flat, but displays a wavy surface, which is the result of diffusion taking place between the bonded surfaces, causing their

1 structures intergrowth. The waviness is more pronounced on the samples processed by
 2 Method B, which used a higher bonding temperature. At the lower bonding temperature
 3 and pressure (850 to 900 °C; 1 MPa) the interface corrugation is about 1-2 μm and it
 4 becomes about 4-5 μm when bonded at a higher temperature and slightly higher
 5 pressure (1000 °C; 1.5MPa). The shape and orientation of the α-Ti lamellar structure, in
 6 the vicinity of interface are similar to the structure in the bulk. Images also show that
 7 incorporation of the reinforcement particles within the matrix stay intact after the
 8 bonding, as seen in Fig.3 and Fig.4. This observation is true regardless of the particles'
 9 morphology: globular in case of TiC and needles and lamellar in case of TiB particles.
 10
 11
 12
 13
 14
 15
 16
 17
 18
 19
 20
 21
 22
 23
 24
 25
 26
 27
 28
 29
 30
 31
 32
 33
 34
 35
 36
 37
 38
 39
 40
 41
 42
 43
 44
 45
 46
 47
 48
 49
 50
 51
 52
 53
 54
 55
 56
 57
 58
 59
 60
 61
 62
 63
 64
 65

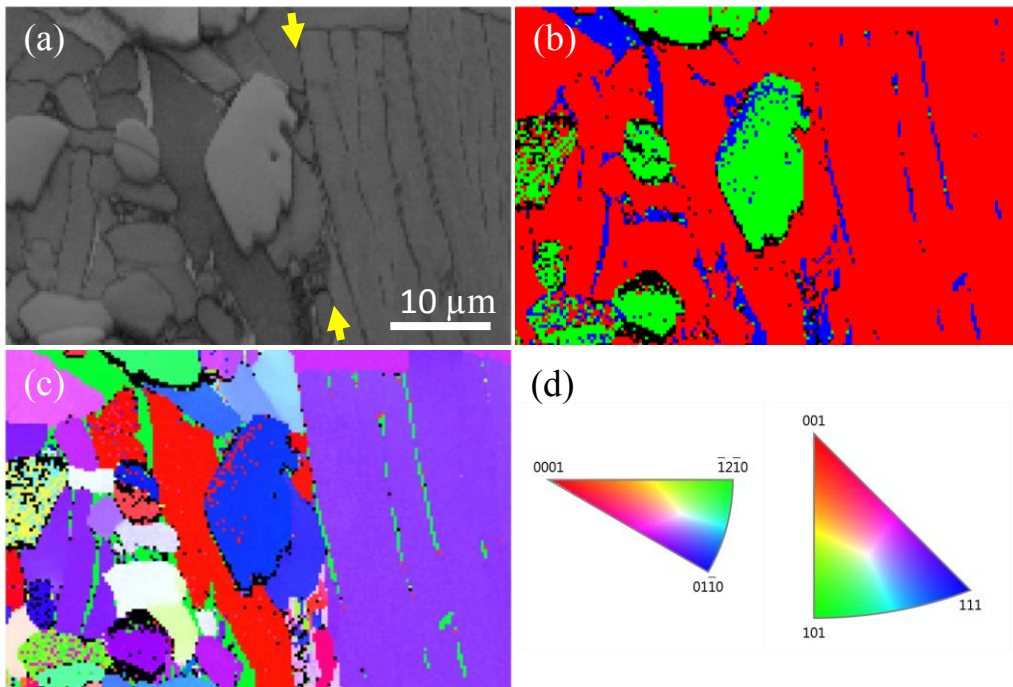


Figure 5. SEM/EBSD results of the DB zone area of TiC-A sample (850 to 900 °C; 1 MPa): band contrast image (a), phase color image (b) and orientation map (c) with stereographic triangles (d) for hexagonal, α-Ti (on the left) and cubic, β-Ti (right) structures. The color is coding different phases in (b): red is for α-Ti, blue is for β-Ti and the green is for TiC. Some defects (noise) of the phase and crystallinity identification are results of not completely removed surface stress on hard TiC inclusions during the sample polishing. Interface between two bonded layers is highlighted with yellow arrows in image A. The α-Ti lamellas are characterized with not deformed structure within the interface. All images are shown at the same magnification.

structure intergrowth as seen in Fig.4 (d). Any structural defects, such as pores, in the vicinity of the reinforcement particles also remained unchanged.

As it was pointed out earlier [17] on DB of Ti-64 alloy, bonding thermal cycles can modify the original Ti-64 lamellar microstructure, transforming the banded structure into an equiaxed structure, due to isothermal annealing below β -transus temperature. This can create a negative effect on mechanical properties. The EBSD orientation maps confirmed the occurrence of cross bond line growth without major plastic deformation of the alloys in vicinity of the interface (Fig.5). In addition, no extensive grain growth or recrystallization was observed close to the bond area. The results of hardness tests measurements within 500 μm across the interface showed hardly any variation in microhardness (Fig.6). Outcomes of the bending tests reveal that all thin slices of the samples made using Method A failed through the composites at

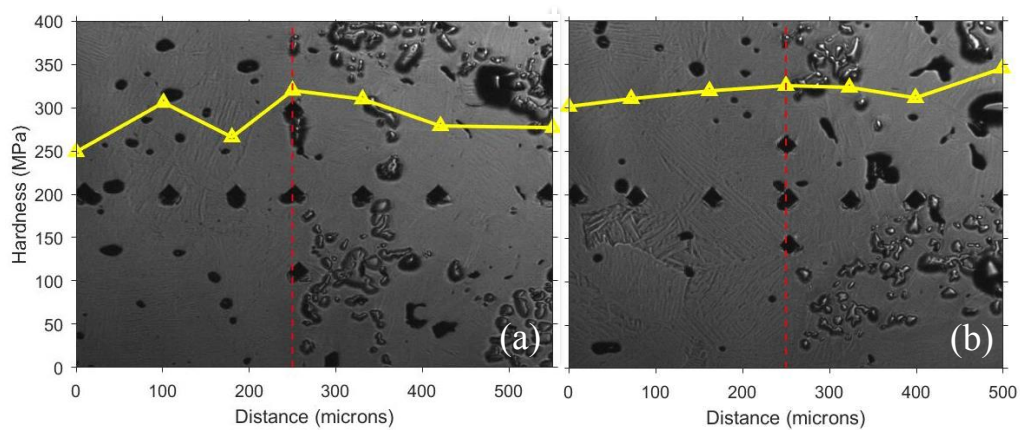


Figure 6. Microhardness test data measured across the bond area of the sample TiC-A (850-900 $^{\circ}\text{C}$; 1 MPa) superimposed and scaled with the LOM images of the bond showing the diamond pyramid imprints after the test. The data show results measured at the edge of the sample (a) and in its center (b). The interface is shown with dotted red line. The values measured right on the interface are average of three measurements.

about few millimetres away from the bond-lines, when subjected to bending force across their joint interfaces.

It is generally accepted [17] that diffusion bonding can be regarded as a process in which the interfacial defects (voids) between two faying surfaces tend to collapse as a result of the diffusion mechanisms which are accelerated by temperature, pressure and time. Elevated pressures favour void collapsing on joints, but tend to produce undesirable macroscopic deformation and affect the cost. Longer bonding times

1 promote interdiffusion but cause grain growth. In both used methods in this study, A
2 and B, no grain size changes were observed within the area of the DB, compared to
3 initial structure. Most likely, in both cases, the temperature was within the two-phase
4 region, and the pores and reinforcement particles facilitated the lack of grain boundaries
5 mobility. Intragrain structure is also restored on the remnants of the primary α -plates
6 during cooling from DB temperature, which was rather slow since no fine secondary α -
7 phase was observed. The partial healing of pores due to heating + applied pressure
8 could possibly take place, however it was not obvious. Generally, the selected
9 experimental parameters do not cause undesirable structural changes (degradation) in
10 the base metal adjacent to the bond interface. Since we do not observe possible negative
11 consequences of tested procession on the structure it appears that an effective
12 compromise between temperature, time and pressure was established in this work
13 leading to consistent quality joints between the Ti-64 alloy and Ti-64 based MMCs. It is
14 worth mentioning that the DB parameters used in this study (in Method A and B) are
15 common for bonding parts made of Ti-64 alloy. Particle reinforcement at ~10% did not
16 appear to alter bonding when compared to the Ti-64 alloy. So, we can conclude that the
17 MMCs with 10% of reinforcement particles has a similar bond-ability to the
18 conventional Ti-64 alloy. However, previous work has shown that the presence of
19 higher amounts of reinforcement particles, e.g. 30-40%, can significantly compromise
20 the bond integrity and its strength [18].

21 **Conclusions**

22 1. DB was successfully used to join parts made of Ti-64 alloy and Ti-64 MMCs with
23 reinforcement particles (10% vol.) of TiB and TiC. Metallographic and EBSD studies,
24 as well as the bending and microhardness tests across the bonds are presented as the
25
26
27
28
29
30
31
32
33
34
35
36
37
38
39
40
41
42
43
44
45
46
47
48
49
50
51
52
53
54
55
56
57
58
59
60
61
62
63
64
65

1 evidence of joint integrity and the lack of microstructure alteration in the vicinity of the
2 joint.
3

4 2. The DB of T-64 and Ti-64 with 10% TiC or TiB was successfully carried out at 900
5 to 1000 °C, with a holding time of 60 minutes under 0.7-1.5 MPa pressure. The bonding
6 cycle did not cause any major change in the grain size and the microhardness of the
7 both materials.
8
9

10 3. Particle reinforcement at ~10% did not appear to alter bonding when compared to the
11 unreinforced Ti-64 alloy.
12
13

14 **Acknowledgements**

15 The following authors SVP, DGS, PEM, OOS, JP acknowledge funding from the
16 NATO Agency Science for Peace and Security (#G5030).
17
18

19 **References**

20 [1] Markovsky PE, Savvakina DG, Ivasishin OM, et al. Mechanical Behaviour of
21 Titanium-Based Layered Structures Fabricated Using Blended Elemental Powder
22 Metallurgy. J Mater Eng Perform. 2019;28(9):5772-5792.
23
24

25 [2] Ivasishin OM, Markovsky PE, Savvakina DG, et al. Multi-Layered Structures of Ti-
26 6Al-4V Alloy and TiC and TiB Composites on Its Base Fabricated Using Blended
27 Elemental Powder Metallurgy. J Mater Process Tech. 2019;269:172–181.
28
29

30 [3] El-Soudani SM, Yu KO, Crist EM, et al. Optimization of blended-elemental powder
31 based titanium alloy extrusions for aerospace applications. Metall Mater Trans.
32 2013:A44. DOI 10.1007/s11661-012-1437-5
33
34

35 [4] Prihodko SV, Markovsky PE, Savvakina DG, et al. Thermo-mechanical treatment of
36 titanium based layered structures fabricated by blended elemental powder metallurgy.
37 Mater Sci Forum. 2018;941:1384-1390.
38
39
40
41
42
43
44
45
46
47
48
49
50
51
52
53
54
55
56
57
58
59
60
61
62
63
64
65

- 1
2
3
4
5
6
7
8
9
10
11
12
13
14
15
16
17
18
19
20
21
22
23
24
25
26
27
28
29
30
31
32
33
34
35
36
37
38
39
40
41
42
43
44
45
46
47
48
49
50
51
52
53
54
55
56
57
58
59
60
61
62
63
64
65
- [5] Bache MR, Tuppen SJ, Voice WE, et al. Novel low cost procedure for fabrication of diffusion bonds in Ti 6/4. *Mater Sci Tech*. 2009;25(1):39-49.
- [6] Rajakumar S, Balasubramanian V. Diffusion bonding of titanium and AA 7075 aluminium alloy dissimilar joints—process modelling and optimization using desirability approach. *Int J Adv Manufacturing Tech*. 2016;86:1095–1112.
- [7] Ghosh SK, Chatterjee S. On the Direct Diffusion Bonding of Titanium Alloy to Stainless Steel. *Mater Manufacturing Proc*. 2010;25:1317–1323.
- [8] Dunford DV, Wisbey A. Diffusion Bonding of Advanced Aerospace Metallic. *Mat Res Soc Symp Proc* 1993;314:39-50.
- [9] Tuppen SJ, Bache MR, Voice WE. A fatigue assessment of dissimilar titanium alloy diffusion bonds. *Int J Fatigue*. 2005;27:651–658.
- [10] Elrefaey A, Tillmann W. Solid state diffusion bonding of titanium to steel using a copper base alloy as interlayer. *J Mater Proc Tech*. 2009; 209:2746–2752.
- [11] Mo DF, Song TF, Fang YJ, et al. A Review on Diffusion Bonding between Titanium Alloys and Stainless Steels. *Advances in Materials Science and Engineering*. 2018;15. <https://DOI.org/10.1155/2018/8701890>
- [12] Nicholas MG. *Joining processes – introduction to brazing and diffusion bonding*. London, Kluwer Academic Publishers; 1998.
- [13] Ashworth MA, Jacobs MH, Davies S. Basic mechanisms and interface reactions in HIP diffusion bonding. *MaterDesign*. 2000;21:351-358.
- [14] Pederson R. *Microstructure and Phase Transformation of Ti–6Al–4V*. Licentiate Thesis, Lulea University of Technology; 2002.
- [15] Shirzadi AA, Kocak M, Wallach ER. Joining stainless steel metal foams. *Sci Tech Welding Joining*. 2004;9(3):277-279.

1 [16] Davies P, Johal A, Davies H. et al. Powder interlayer bonding of titanium alloys:
2 Ti-6Al-2Sn-4Zr-6Mo and Ti-6Al-4V. Int J Adv Manuf Tech. 2019;103:441–452.
3

4 [17] Carrión JG. A Study of Low Temperature Diffusion Bonding Processing of TI-
5 6AL-4V Alloy for Reducing Costs in SPF/DB Structures. RTO-MP-069 (II), Cost
6 Effective Application of Titanium Alloys in Military Platforms, Loen, Norway, 7-11
7 May 2001.
8
9

10 [18] Shirzadi AA, Wallach ER. New approaches for the TLP diffusion bonding of
11 aluminium metal matrix composites. Mater Sci Tech. 1997;13(2):135-142.
12
13
14
15
16
17
18
19
20
21
22
23
24
25
26
27
28
29
30
31
32
33
34
35
36
37
38
39
40
41
42
43
44
45
46
47
48
49
50
51
52
53
54
55
56
57
58
59
60
61
62
63
64
65

Figure Captions

1
2
3 Figure 1. Sample TiB-B2 after DB. The area of the joint is in the middle of the rod.

4
5 Slight oxidation is observed at about 15 mm distance on both sides from the interface
6
7
8 between bond samples.
9

10
11 Figure 2. Image of the sample TiC-A demonstrate some of macro defects of the bonding
12 extended inside the sample on about 100-150 μm from the edge (a), whereas rest of the
13 sample reveal consistency and no visible defects of the bonding along the interface (b).
14
15
16

17
18 Figure 3. SEM images of the interface resulted on DB of the TiC-A sample processed at
19 bonding temperature between 850 to 900 $^{\circ}\text{C}$ and 1 MPa bonding pressure. The area
20 boxed in (a) is shown in (b).
21
22
23
24
25
26

27
28 Figure 4. Images of the bond area of the TiC-B2 (a, b) and TiB-B2 (c, d) processed at
29 1000 $^{\circ}\text{C}$ for 60 minutes at a stress of 1.5MPa. Images (b) and (d) shows boxed areas in
30
31
32 (a) and (c) correspondingly.
33
34
35

36
37 Figure 5. SEM/EBSD results of the DB zone area of TiC-A sample (850 to 900 $^{\circ}\text{C}$; 1
38 MPa): band contrast image (a), phase color image (b) and orientation map (c) with
39 stereographic triangles (d) for hexagonal, α -Ti (on the left) and cubic, β -Ti (right)
40 structures. The color is coding different phases in (b): red is for α -Ti, blue is for β -Ti
41 and the green is for TiC. Some defects (noise) of the phase and crystallinity
42 identification are results of not completely removed surface stress on hard TiC
43 inclusions during the sample polishing. Interface between two bonded layers is
44 highlighted with yellow arrows in image (a). The α -Ti lamellas are characterized with
45 not deformed structure within the interface. All images are shown at the same
46
47
48
49
50
51
52
53
54
55
56
57
58
59 magnification.
60
61
62
63
64
65

Figure 6. Microhardness test data measured across the bond area of the sample TiC-A (850- 900 °C; 1 MPa) superimposed and scaled with the LOM images of the bond showing the diamond pyramid imprints after the test. The data show results measured at the edge of the sample (a) and in its center (b). The interface is shown with dotted red line. The values measured right on the interface are average of three measurements.

1
2
3
4
5
6
7
8
9
10
11
12
13
14
15
16
17
18
19
20
21
22
23
24
25
26
27
28
29
30
31
32
33
34
35
36
37
38
39
40
41
42
43
44
45
46
47
48
49
50
51
52
53
54
55
56
57
58
59
60
61
62
63
64
65



Figure 1. Sample TiB-B2 after DB. The area of the joint is in the middle of the rod. Slight oxidation is observed at about 15 mm distance on both sides from the interface between bond samples

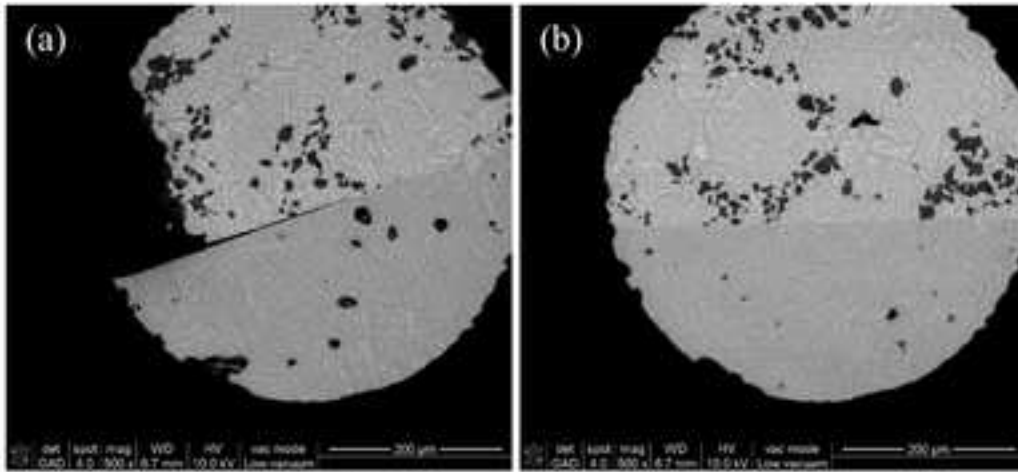


Figure 2. Image of the sample TiC-A demonstrate some of macro defects of the bonding at about 100-150 μm close to the edge of the sample (a), whereas rest of the sample reveal consistency and no visible defects of the bonding along the interface (b).

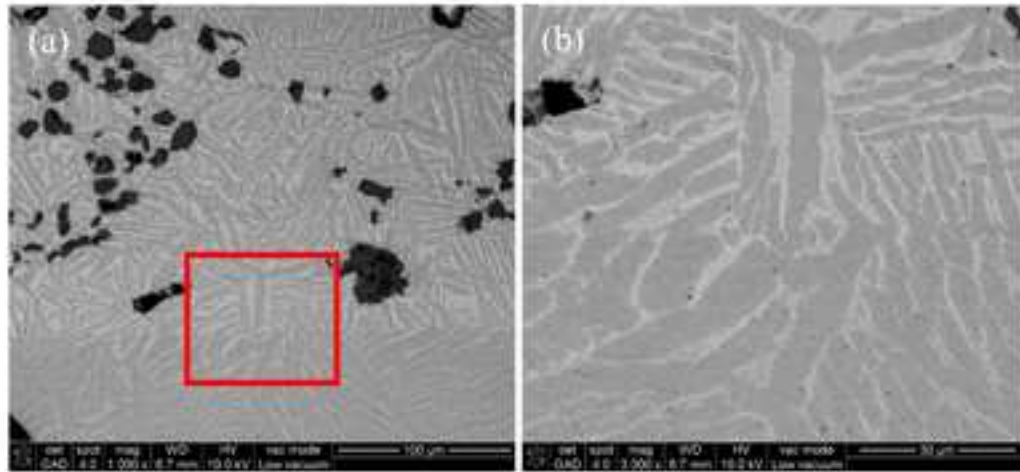


Figure 3. SEM images of the interface resulted on DB of the TiC-A sample processed at bonding temperature between 850 to 900 °C and 1 MPa bonding pressure. The area boxed in (a) is shown in (b).

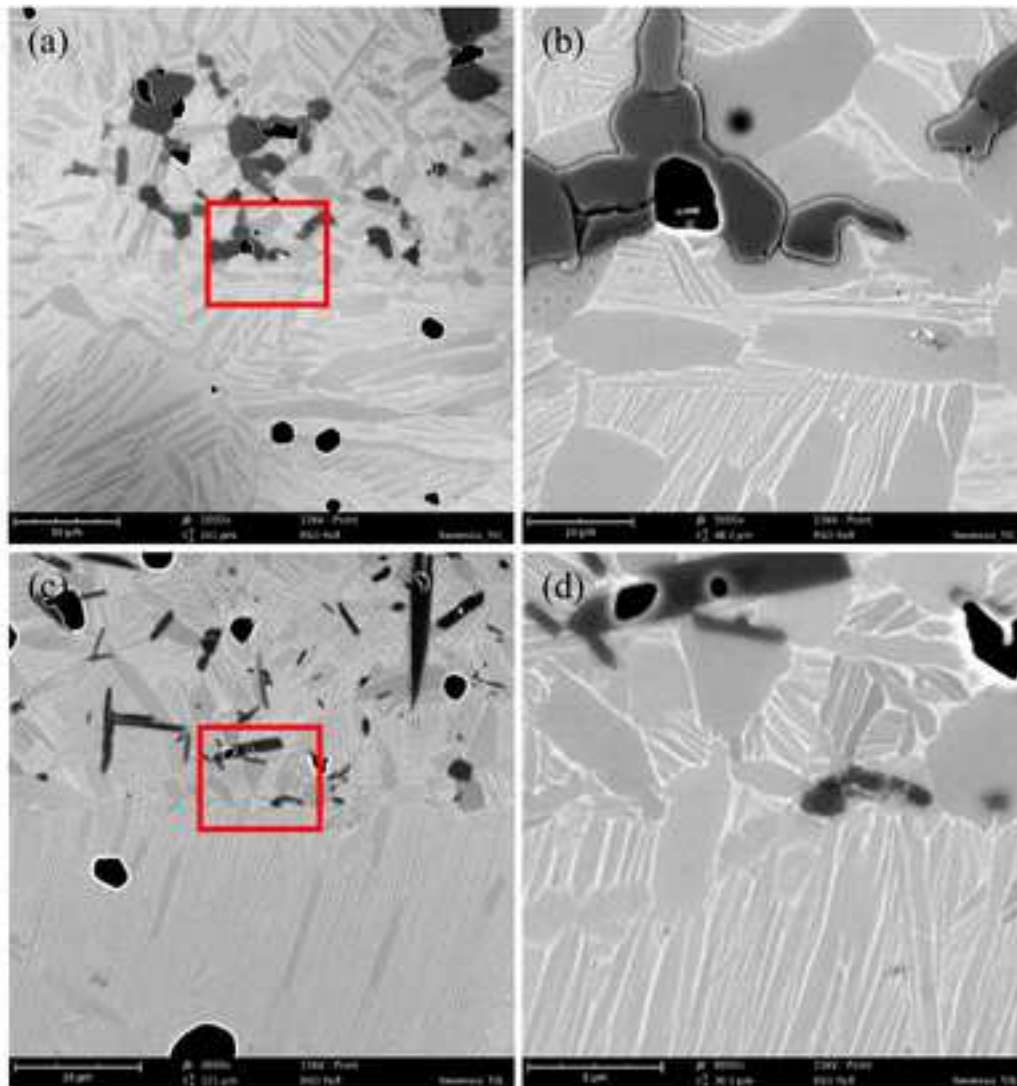


Figure 4. Images of the bond area of the TiC-B2 (a, b) and TiB-B2 (c, d) processed at 1000 °C for 60 minutes at a stress of 1.5MPa. Images (b) and (d) shows boxed areas in (a) and (c) correspondingly.

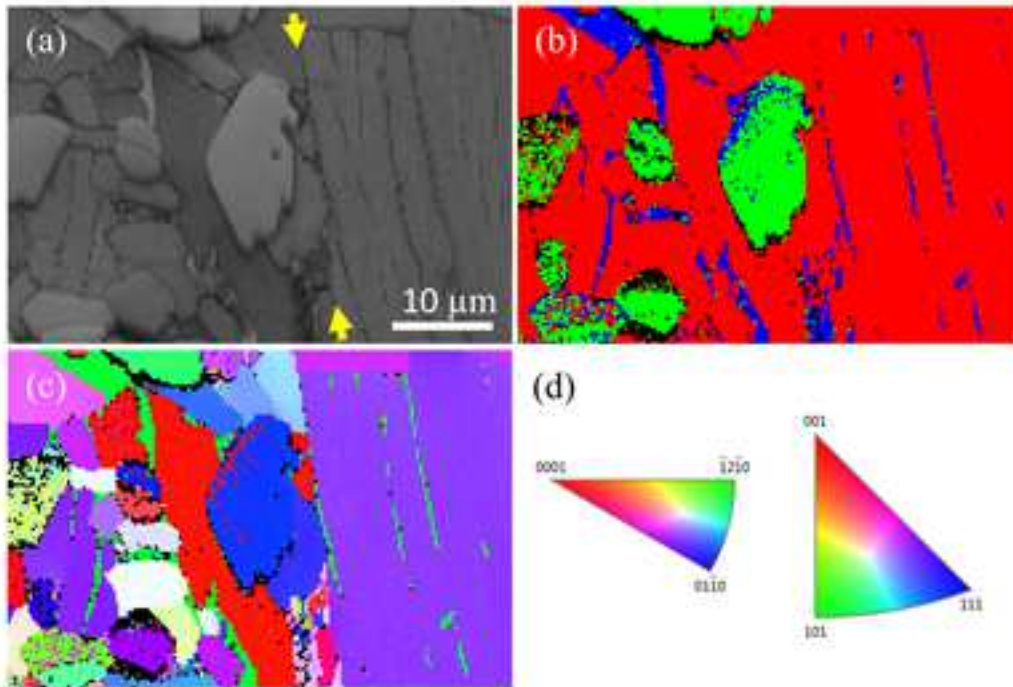


Figure 5. SEM/EBSD results of the DB zone area of TiC-A sample (850 to 900 °C; 1 MPa): band contrast image (a), phase color image (b) and orientation map (c) with stereographic triangles (d) for hexagonal, α -Ti (on the left) and cubic, β -Ti (right) structures. The color is coding different phases in (b): red is for α -Ti, blue is for β -Ti and the green is for TiC. Some defects (noise) of the phase and crystallinity identification are results of not completely removed surface stress on hard TiC inclusions during the sample polishing. Interface between two bonded layers is highlighted with yellow arrows in image A. The α -Ti lamellas are characterized with not deformed structure within the interface. All images are shown at the same magnification.

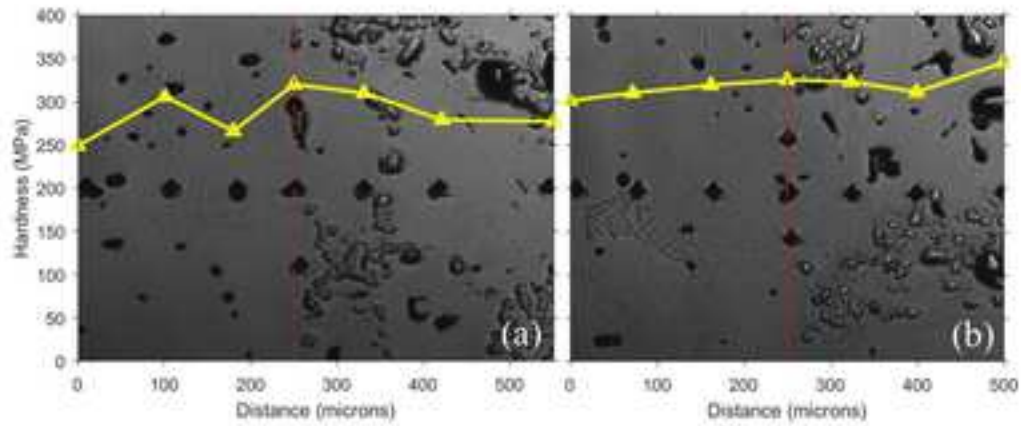


Figure 6. Microhardness test data measured across the bond area of the sample TiC-A (850- 900 °C; 1 MPa) superimposed and scaled with the LOM images of the bond showing the diamond pyramid imprints after the test. The data show results measured at the edge of the sample (a) and in its center (b). The interface is shown with dotted red line. The values measured right on the interface are average of three measurements.